Preparation of a Polymeric Membrane with a Fine Porous Structure by Dry Casting

Jae-Kyung Kim, Kentaro Taki, Shinsuke Nagamine, Masahiro Ohshima

Department of Chemical Engineering, Kyoto University, Kyoto 615-8510, Japan

Received 28 May 2008; accepted 8 August 2008
DOI 10.1002/app.29348
Published online 25 November 2008 in Wiley InterScience (www.interscience.wiley.com).

ABSTRACT: We prepared a polymeric membrane with a fine porous structure from polystyrene (PS), poly(ethylene glycol) (PEG), and solvent solutions by exploiting the phase separation induced in the course of dry casting. To determine the effect of the drying rate and phase separation on the developed porous structure, six different solvents, including toluene, chlorobenzene, tetrahydrofuran, methyl ethyl ketone, 1,4-dioxane, and chloroform, were used. The pore size and density drastically changed with the different solvents and drying conditions. The polymer concentration at the onset of the phase separation into PEG-rich and PS-rich phases also strongly affected the cellular structure. The solubility of PEG into PS and the solvent solutions changed the concentration, which corresponded to the viscosity of the PS-rich solution at the onset of the phase separation. The higher solubility of PEG in the solutions delayed the onset of phase separation during drying and increased the viscosity. The higher viscosity and the higher drying rate prevented the phase-separated PEG domains from coalescing and made the resulting pore size smaller and the pore density larger. The finest porous structure, with a pore size of approximately 1 μm and a pore density of 0.08 $1/\mu m^2$, was prepared from PS/PEG and a 90 wt % chloroform solution. © 2008 Wiley Periodicals, Inc. J Appl Polym Sci 111: 2518–2526, 2009

Key words: macroporous polymers; membranes; morphology; phase separation; polystyrene

INTRODUCTION

Polymeric porous membranes with fine pores in the range from the micrometer scale to the submicrometer scale have attracted much attention for various applications, such as membrane separation and purification,[1] solid supports for sensors and catalysts,[2] scaffolds for biological cells,[3] low-dielectric-constant materials for microelectronic devices,[4] and battery separators in fuel cells and lithium ion batteries.[5] Polymeric porous membranes can be prepared by several methods, such as sintering,[6] stretching,[7] the removal of inorganic salts, carbon dioxide foaming,[8] and the phase separation of polymer solutions.[9–11] Recently, phase separation[12–17] in immiscible polymer blend solutions has been of great interest because of the simplicity and cost efficiency of the process. Phase separation in polymer blends is induced by the evaporation of the solvent (solvent quenching).[18,19] A morphology with domains dispersed in a continuous phase is generally developed by the phase separation.[20] Several studies on polymeric porous membranes prepared by the exploitation of the phase separation of immiscible polymer blends have been carried out. Cui and Han[21] developed a porous film from polystyrene (PS)/poly(2-vinylpyridine) via the dry casting of an ethyl benzene/polymer solution. Walheim et al.[22] prepared a porous thin film of PS and poly(methyl methacrylate) by the spin coating of polymer–solvent solutions. Nakane et al.[23] fabricated a porous membrane from poly(L-lactic acid), poly(ethylene glycol) (PEG), and chloroform solution by dry casting. Phase separation in polymer blends has often been used to prepare porous materials, and the formation mechanism of some porous structures created from polymer blend solutions has been identified. It is known that the dispersed domain (droplet) size and its density can be changed by the coalescence of domains during phase separation,[24–27] and the process often results in a low domain density and large domain size.[28] Various factors, such as solvent type,[29] concentration,[30] molecular weight of the polymer,[31–33] and weight ratios of the polymers,[23,29,33] for the determination of the dispersed domain size and the density have been identified. However, there still remains a great challenge in the control of the pore size and pore density and clarification of the formation mechanisms of porous structures because of the versatility of polymer blend morphologies.

In our previous study,[31] we examined the formation mechanism of porous structures on the surface

Correspondence to: M. Ohshima (oshima@cheme.kyoto-u.ac.jp).

of film made from a ternary component solution: PS/PEG and a toluene solution. We speculated that the phase separation into a PEG-rich domain and PS-rich phases and a successively induced secondary phase separation in the PEG-rich domain (i.e., polymer–solvent phase separation) created the unique porous structure. In this study, we further investigated the PS/PEG/solvent systems in terms of the controllability of pore size, pore density, and location of the pores in the film. Using six different solvents in the PS/PEG polymer blend, we investigated the effects of polymer solubility in the solvents and drying rate on the porous structure. Furthermore, the formation mechanism of the structure was also examined.

EXPERIMENTAL

Materials

PS and PEG were purchased from Aldrich Chemical Co. (USA) and Wako Pure Chemicals Industries, Ltd. (Japan), respectively. The weight-average molecular weight (M_w), number-average molecular weight (M_n), and polydispersity (M_w/M_n) of these polymers were measured by gel permeation chromatography (Shimadzu, model DGU-20A_3; column: Shodex GPC KF-806L; eluent: chloroform). The retention time and molecular weight were calibrated with PS standards. Six different organic solvents, including dehydrated toluene, dehydrated tetrahydrofuran (THF), dehydrated methyl ethyl ketone (MEK), dehydrated chlorobenzene, dehydrated 1,4-dioxane, and dehydrated chloroform (Wako Pure Chemicals Industries, purity = 99.5%) were used without further purification. The characteristics of the materials used in this study are listed in Table I.

Membrane preparation

PS and PEG were blended at a weight ratio of 70/30 and dissolved into the six different solvents at a 10 wt % polymer concentration. The polymer solution was cast by a microinjector onto an aluminum Petri dish, which had a radius of 2.1 cm and a depth of 0.5 cm. We controlled the film thickness by changing the amount of injected solution. The volume of solution injected was 100 μL in the nominal case. The initial thickness of solution was about 300 μm, and all of the samples were prepared with the same amount of solution. The casting and drying were performed in a thermocontrolled incubator (Eyela, LTI-600SD, Japan), where the Petri dish was placed in a 17 × 17 × 17 cm^3 plastic container under nitrogen (purity = 99.9%) with purging at 30°C. Nitrogen gas was introduced into the container from the vertical direction to the solution surface. The humidity and temperature in the incubator were measured by a hydrothermograph (SK-L200T II, Sato Keiryoki Mfg. Co., Ltd.).

Observation of the membrane morphology

The porous structure of the obtained films was observed by scanning electron microscopy (SEM; Tiny-SEM 1540, Technex Lab Co., Ltd., Japan) with the treatment of gold–palladium sputter coating under a vacuum atmosphere. For the density calculation, we counted the number of pores observed in a micrograph of the cross-sectional area of the film and divided the number by the area of the cross section.

Cloud point measurement

We determined the cloud point temperatures by monitoring the intensity of the laser beam transmitted through the solution. A cell containing the sample solution was immersed in a thermostatically controlled water bath. At first, the temperature was increased until the solution became homogeneous, and then, it was decreased at a rate of 0.1°C/min under continuous stirring until the solution became turbid with the phase separation. A more detailed description of these techniques can be found elsewhere.[31]

TABLE I
Characteristics of PEG, PS, and the Various Solvents

Material	M_w	M_n	M_w/M_n	Vapor pressure (mmHg) at 20°C	δ ($MPa^{0.5}$)
Polystyrene (PS)	222,000	99,000	2.24		18.6[35]
Polyethylene glycol (PEG)	280	260	1.07		26.1[36]
Chlorobenzene				12	19.4[35]
MEK				71	19[35]
THF				129	18.6[35]
1,4-Dioxane				27	20.5[35]
Toluene				22	18.2[35]
Chloroform				159	19[35]

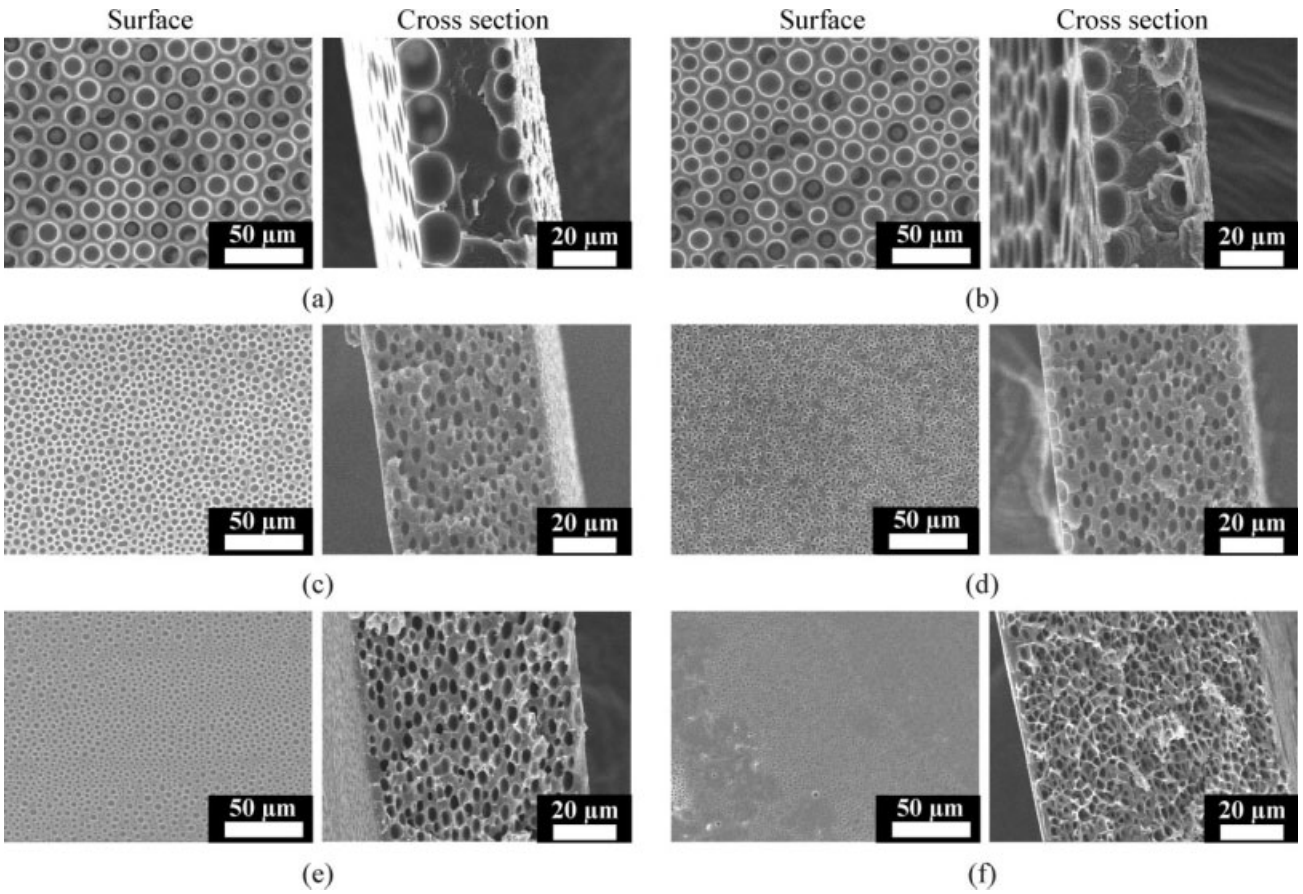

Figure 1 SEM micrographs of the surfaces and cross-sectional areas of PS/PEG200 (70/30 w/w) cast from a 90 wt % solvent under a 3-L/min N_2 flow: (a) toluene, (b) chlorobenzene, (c) THF, (d) MEK, (e) 1,4-dioxane, and (f) chloroform.

Measurement of the drying rate

The solution was dropped into an aluminum Petri dish mounted on an electronic balance and allowed to evaporate under a nitrogen purge. The weight change in the solution was measured by the electronic balance to determine the drying rate. The drying rate was changed for the different solvents because of their differences in vapor pressure and the change in nitrogen flow rate. To conduct the drying at low drying rates, we realized the solvent annealing conditions by placing a lid on the sample Petri dish.

Viscosity measurement

The shear viscosity of the polymer solution was measured with an ARES mechanical spectrometer (Rheometric Science, USA) with a steady-state sweep test mode. A couette-type geometry, with a 50-mm cup diameter, 48-mm bob diameter, and a 25-mm bob length, was used for the measurements. The shear rate and temperature were set at 100 L/s and 30°C, respectively.

RESULTS

Formation of the porous structure in the PS/PEG blend membrane film

Six homogeneous solutions of PS/PEG blends with different solvents were prepared. All of the solutions were made at the 70/30 PS/PEG weight ratio and at 10 wt % of polymer concentration. The polymer solutions were then cast onto an aluminum Petri dish and dried as described in the previous section. For a reference, a homogeneous solution of PS alone with chloroform solvent was prepared and dried with the same procedure. Figure 1 shows the SEM micrographs of the surface and the cross-sectional area of the resulting membrane films made from the six different solutions. Figure 2 shows the SEM micrograph of the cross-sectional area of the resulting PS film. As shown in Figures 1 and 2, the porous structure was well formed in all of the polymer blend films but not in the film of PS alone. The smallest pore diameter, which was about 1.5 μm, was observed in the membrane films made from chloroform solution. A comparison of the micrographs in Figure 1 with that in Figure 2 clearly shows that the presence of

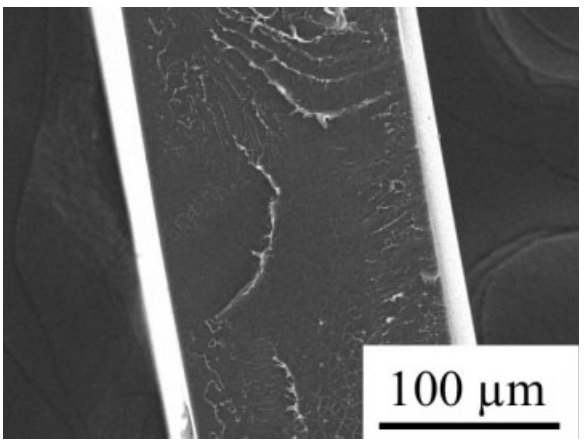

Figure 2 SEM cross-sectional micrograph of PS cast from a 90 wt % chloroform solution under 3-L/min N_2 purging.

the PEG composition affected the morphology of the polymer blend membrane. In other words, the film fabricated without PEG had no porous structure, whereas the films made from the PS/PEG solutions showed fine porous structures.

As illustrated in Table I, the solubility parameters of PS and PEG were different, and the solubilities of PS and PEG in the solvents were different as well. The solubility parameters of the polymers and solvents indicated that all of the solvents used in this study were poor for PEG. Thus, in the course of the drying of the polymer solutions, the phase separation into PEG-rich and PEG-poor (i.e., PS-rich) phases occurred. The PEG-rich phase dispersed domain formed droplets, and the PEG-poor phase became a matrix where the PS and solvent coexisted as a single-phase solution. In our previous study on the PS/PEG/toluene system,[31] we determined that secondary phase separation followed in the PEG droplets, which was induced by further solvent evaporation, and formed solvent-rich and PEG-rich domains within the droplets. The solvent evaporation and secondary phase separation created the pores in the film. It was also evident that porous structure was created by the presence of the PEG composition in solution, and the phase separation of the PEG rich phase was induced before complete solidification by drying. However, the pore size and pore location in the film were different with the different kinds of solvent.

Effect of the solvent on the formation of the porous structure in the PS/PEG blend membrane

As we have discussed, the pore size and density of the pores in the membrane were different with the various solvents. The pore size and the density of the cross-sectional area measured in the SEM micrographs are shown in Figure 3. The pore size became largest and the density became smallest in the film made from the toluene solution, and the size became smallest and the density became largest in the film made from the chloroform solution. Furthermore, it is interesting that, as illustrated in Figure 1, few pores were created inside the membrane films made from the toluene and chlorobenzene solutions. Porous structures were created inside the films made from THF, MEK, and 1,4-dioxine solutions, and their structures were similar to each other. Their respective pore sizes and densities were similar: 2.7 μm and 0.03 $1/\mu m^2$ for THF, 2.6 μm and 0.03 $1/\mu m^2$ for MEK, and 2.8 μm and 0.03 $1/\mu m^2$ for 1,4-dioxane. They also showed similar closed-cell structures, and the locations of the pores were inside the films. Moreover, the PS/PEG membrane film made from the chloroform solution showed a fine porous structure, with a pore size and density of 1.56 μm and 0.08 $1/\mu m^2$, respectively.

As discussed, the different solvents changed the pore size and the density of the pores. The resulting porous structures could be classified into two types in terms of size and location: (1) over 10 μm size pores on the surface and at the interface of the substrate with few pores inside the film [Fig. 1(a,b)] and (2) single micrometer size porous structures inside the film and several micrometer size pores on the interface and surface [Fig. 1(c–f)].

The resulting porous structures indicated that the occurrence of phase separation alone could not explain the formation mechanism of the pore size and the density of the pores. The factors controlling the process, such as the drying rate and change in viscosity of the polymer solution, also affected the porous structure.

We measured the drying rate in each solution by weighing the solution over the course of drying, and the solubility of PEG in each solvent was estimated by the Flory–Huggins interaction parameter (χ). The

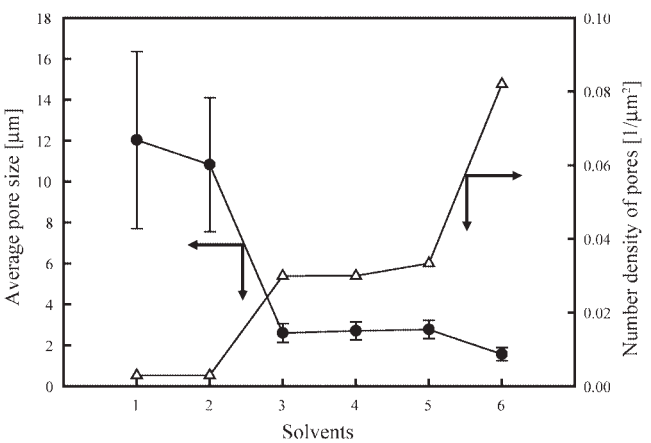

Figure 3 Pore size and number density of the pores in each solvent: (1) toluene, (2) chlorobenzene, (3) THF, (4) MEK, (5) 1,4-dioxane, and (6) chloroform.

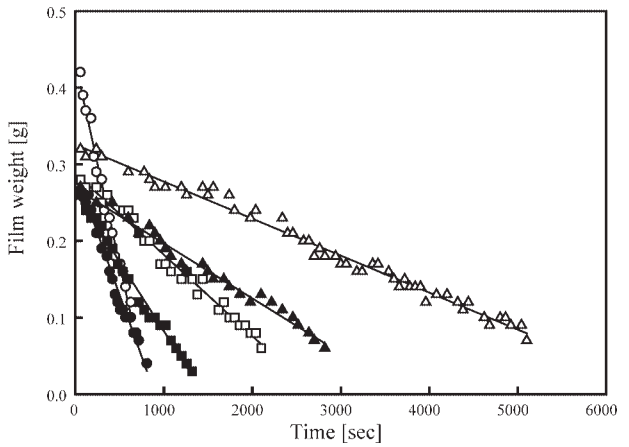

Figure 4 Drying rates for several polymer blend/solvent systems: (○) chloroform, (●) THF, (□) 1,4-dioxane, (■) MEK, (△) chlorobenzene, and (▲) toluene.

interaction parameters were calculated from the solubility parameters of PEG and the solvents by the following equation:

$$\chi = \frac{V_i}{RT}(\delta_i - \delta_j)^2 + \beta \quad (1)$$

where V_i is the molar volume of the solvent; δ_i and δ_j are the Hildebrand solubility parameters for the solvent and polymer, respectively; R is the gas constant; and T is the absolute temperature.[34] β corresponds to the entropic component, and a value of 0.34 is used for nonpolar systems. The interaction parameters in this study were calculated without an entropic component ($\beta = 0$) because of the polarity of PEG.[34]

Figure 4 shows some experimental results of the drying rate. The value of the drying rate was calculated from the initial slope of the weighing curve against drying time. The measured drying rate and the calculated χ values are listed in Tables II and III, respectively. Figure 5 plots the average pore size and density of the pores in the cross-sectional area of the polymer blend/solvent systems in the coordinate system of drying rate and χ between its solvent and PEG. Figure 5 clearly shows that the higher drying rate and lower χ made the porous structure in the membranes finer; that is, they made the pore size smaller and the density larger.

DISCUSSION

In the course of drying a ternary composition polymer solution, solvent evaporation induces phase separation. When slow drying proceeds, the solvent concentration decreases from the surface, and phase separation occurs from the surface. Because of the higher solubility of PS in all of the solvents used in this study, PEG was phase-separated at the solution surface and formed droplets. As drying proceeded, the solvent concentration profile propagated inside the solution, and PEG-rich domains were created inside the solution and coalesced. The growth rate of the PEG-rich domains was affected by the drying rate and the solubility of PEG in the solvent. Thus, when fast drying proceeded, the increase in the drying rate increased the polymer concentration and the viscosity of the PS-rich phase (matrix phase) quickly. A high polymer concentration and high viscosity of the solution suppressed the coalescence of the PEG-rich domains and made the domain size smaller and increased the density of the domains in the membrane. To confirm the controllability of pore size and the number density of the pores by the drying rate, the PS/PEG/toluene and PS/PEG/chloroform systems were further investigated by variation of the drying rate. The drying rate was changed through a change in the flow rate of nitrogen. To attain a very slow drying rate, drying was carried out under a solvent-annealing atmosphere and by the sealing of the sample in the Petri dish. The results are listed in Table II, and the SEM micrographs corresponding to each drying rate are shown in Figure 6. Figure 7 shows the changes in the pore size and density of the pores measured from Figure 6. As shown in Figure 7, an increase in the drying rate made the pore size smaller and increased the density of the pores. The results agree with the results of the pore

TABLE II
Drying Rates of the PS/PEG200/Solvent Systems

System	Flow rate of nitrogen	Drying rate [g/(cm^2 s)]
PS/PEG/toluene	3 L/min	2.29×10^{-5}
PS/PEG/toluene	6.5 L/min	3.63×10^{-5}
PS/PEG/toluene	9 L/min	4.36×10^{-5}
PS/PEG/chloroform	3 L/min	19.07×10^{-5}
PS/PEG/chloroform	2 L/min	16.62×10^{-5}
PS/PEG/chloroform	0.75 L/min	9.99×10^{-5}
PS/PEG/chloroform	3 L/min (under solvent annealing)	3.41×10^{-5}
PS/PEG/chlorobenzene	3 L/min	1.54×10^{-5}
PS/PEG/THF	3 L/min	10.28×10^{-5}
PS/PEG/MEK	3 L/min	5.76×10^{-5}
PS/PEG/1,4-dioxane	3 L/min	3.37×10^{-5}

TABLE III
χ Values of the Solvents and Polymers

Material	Molar volume (cm^3/mol)	$\chi_{PEG-solvent}$ at 30°C	$\chi_{PS-solvent}$ at 30°C
Toluene	106.8	2.64	0.35
Chlorobenzene	102.1	1.81	0.37
Chloroform	80.7	1.61	0.35
THF	81.7	1.82	0.34
MEK	90.1	1.80	0.35
1,4-Dioxane	85.7	1.07	0.46

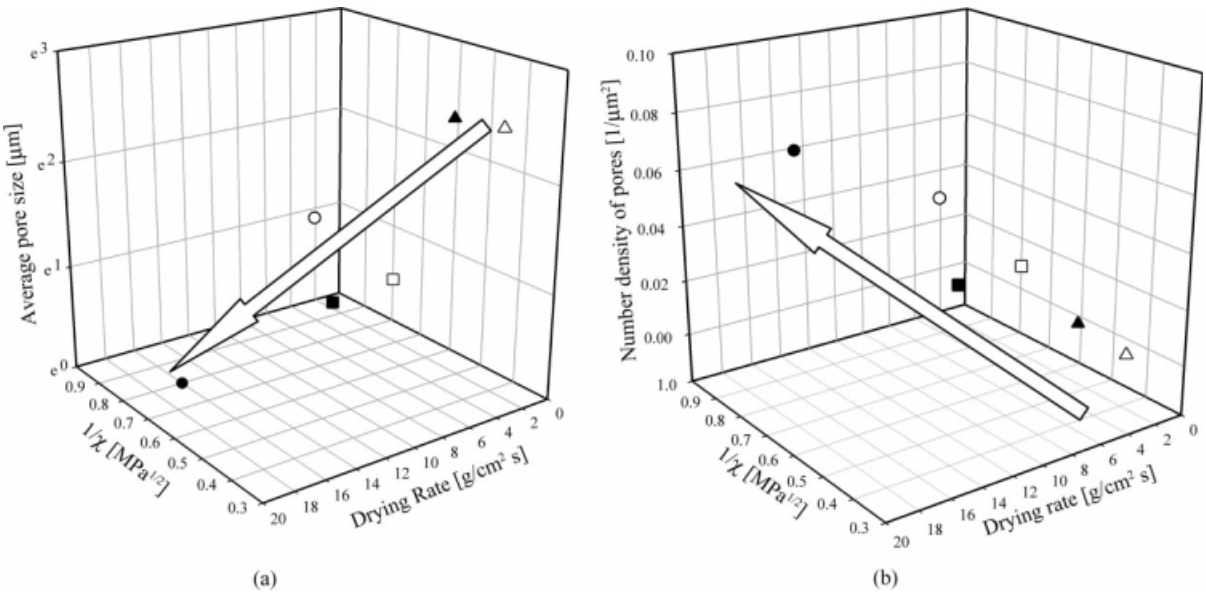

Figure 5 (a) Average pore size and (b) number density of the pores in the polymer blend/solvent systems on a diagram of the drying rate and χ between the solvent and PEG: (△) toluene, (▲) chlorobenzene, (□) MEK, (○) 1,4-dioxane, (■) THF, and (●) chloroform.

size and density shown in Figure 5. Therefore, it was obvious that the pore size and density of the pores in the membrane could be controlled by the drying rate.

The effect of the solubility of PEG in the solvent on the controllability of the pore size and density of the pores was analyzed by means of χ. χ corresponded to the solubility of the polymer in the solvent. A polymer was considered to be miscible in a solvent when χ was lower than 0.5.[35] It is well known that the smaller the value of χ is, the higher the solubility of the polymer in the solvent is. As listed in Table III, the solubility of PEG200 in the solvent increased from 1,4-dioxane to chloroform to MEK to THF to chlorobenzene to toluene. When the solubility of PEG in the solvent increased, the

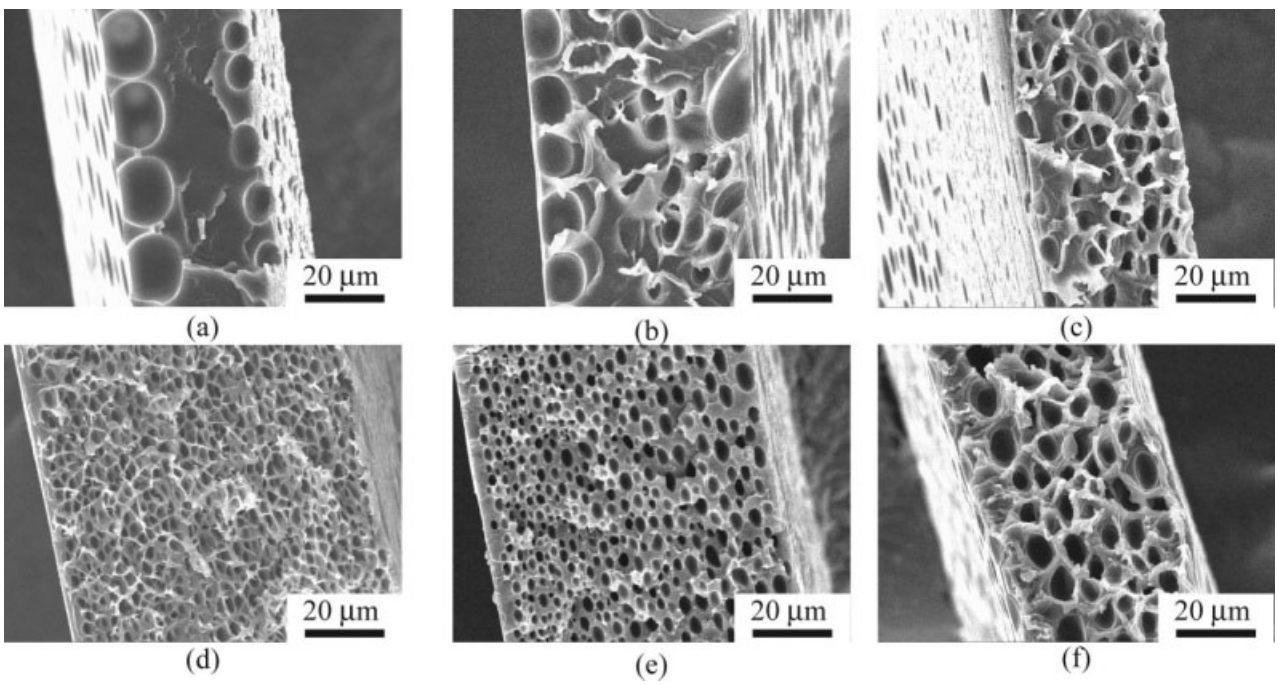

Figure 6 SEM micrographs of cross-sectional areas of films whose drying rates were controlled by the flow of N_2 and a cover: (a) 3 L/min, (b) 6.5 L/min, and (c) 9.5 L/min for a toluene solution and (d) 3 L/min, (e) 0.75 L/min, and (f) a cover for a chloroform solution.

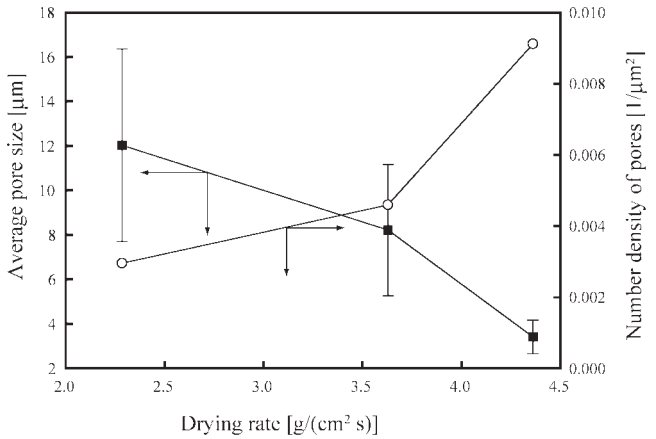

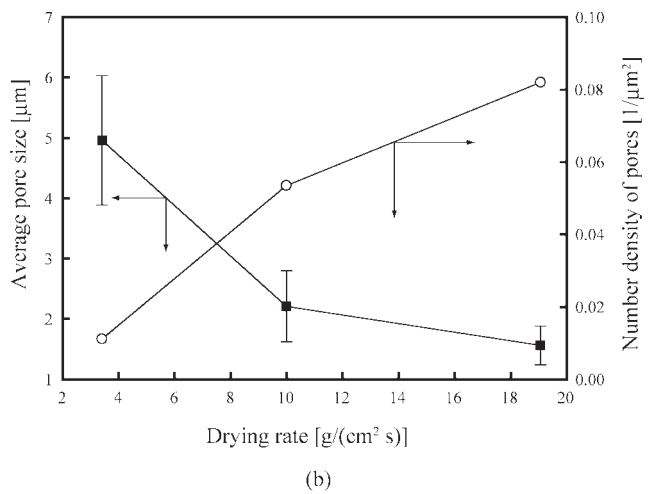

Figure 7 Changes in the pore size and density of the pores: (a) PS/PEG/toluene and (b) PS/PEG/chloroform.

polymer concentration at the onset of the PEG phase separation increased. The cloud point temperatures of the PS/PEG200/toluene, PS/PEG200/chlorobenzene, and PS/PEG200/chloroform solutions were measured experimentally by the variation of the polymer concentration in solution. The resulting cloud point temperatures are plotted in Figure 8. The concentrations of the PS/PEG200/solvent systems at the cloud point at 30°C, whose PS/PEG weight ratios were 70/30, were calculated from Figure 8 and are plotted in Figure 9. As shown in Figure 9, the PEG concentrations in the ternary solutions at the onset of the PEG phase separation were 6.53 for PS/PEG200/toluene, 8.7 wt % for PS/PEG200/chlorobenzene, and 9.75 wt % for PS/PEG200/chloroform. In other words, the concentrations of PS in the ternary solution at the onset of the PEG phase separation were 15.23 wt % for PS/PEG200/toluene, 20.3 wt % for PS/PEG200/chlorobenzene, and 22.75 wt % for PS/PEG200/chloroform. This means that the increase in PEG concentration in the solution at the onset of phase

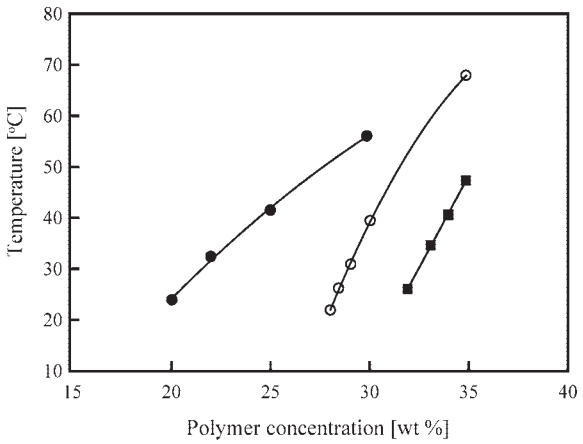

Figure 8 Cloud point temperatures of PS/PEG/solvent solutions versus the polymer concentration in solution with a PS/PEG weight ratio of 70/30 wt %: (●) toluene, (○) chlorobenzene, and (■) chloroform.

separation made the polymer concentration of the PS-rich phase higher. Figure 10 shows the viscosity of the PS/toluene, PS/chlorobenzene, and PS/chloroform solutions at 30°C and clearly shows that the solution viscosity increased with increasing PS concentration. Thus, the increase in the solubility of PEG in the solvent increased the polymer concentration, and the viscosity of the solutions at the onset of phase separation increased. The higher viscosity of the solution could suppress the coalescence of the PEG-rich domain after phase separation. Therefore, the pore size decreased with increasing solubility of PEG in the solvent. Because of the mass balance of PEG, the density of the pores became larger as the

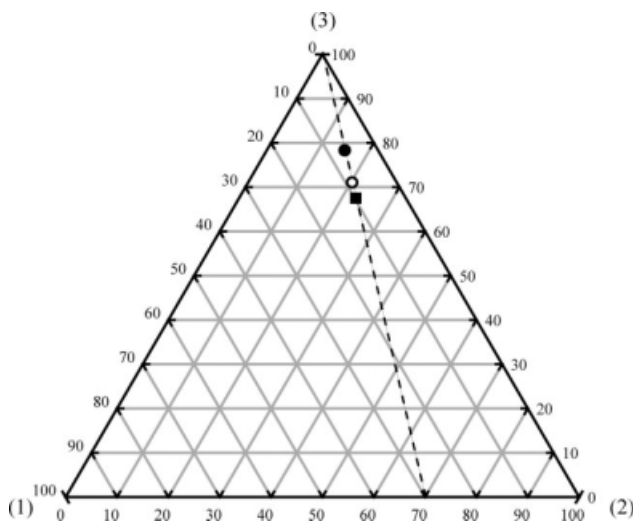

Figure 9 Phase diagram of PEG (1)/PS (2)/solvent (3) solutions at 30°C. The dashed line shows the PS/PEG polymer blend with a 70/30 wt % PS/PEG weight ratio; the cloud point concentrations at 30°C are shown for (●) toluene, (○) chlorobenzene, and (■) chloroform.

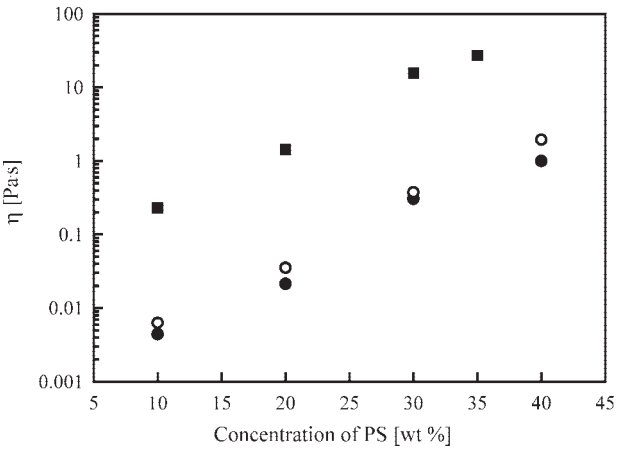

Figure 10 Measured steady-state viscosity (η) as a function of the concentration of PS at 30°C: (●) PS/toluene, (○) PS/chlorobenzene, and (■) PS/chloroform.

pore size became smaller. Thus, the frequency of the coalescence of the PEG-rich domain was controlled by the viscosity of the matrix (the PS-rich phase) at the onset of PEG phase separation, that is, the solubility of PEG in the solvent.

The formation mechanism of the fine porous structure in the membrane is schematically illustrated in Figure 11. As drying proceeded, the phase separation of the PEG-rich domains occurred from the surface and progressed toward the inside of the film, and the film thickness decreased.

When there was a higher drying rate with a higher solubility of PEG in the solvent system, the PEG-rich domains created inside of the film could not easily coalesce because of the higher viscosity of the matrix at the onset of phase separation. Therefore, the PEG-rich domains remained in the interior of the membrane, and a fine porous structure was created in the PEG droplets by secondary phase separation in the membrane.

On the other hand, when the drying rate was lower and the solubility of PEG in the solvent was lower, the coalescence of the phase-separated PEG-rich domains was very active because of the lower viscosity (low concentration) of the matrix. As drying continued, the PEG-rich domains created in the interior of the membrane could easily coalesce and create large droplets. The droplets were attracted to the surface or interface of the membrane because of the surface energy and the density of PEG. The density of PEG was larger than those of PS and solvents (the densities of PEG, PS, and toluene were 1.11, 1.04, and 0.87 g/cm^3, respectively). The PEG-rich droplets precipitated at the air–solution surface floated on the surface of the solutions by a balance of surface tensions[13,31] but flowed down to the bottom because of gravity when the balance was broken. During drying, some of the precipitated droplets descended and created pores at the substrate side. Therefore, as shown in Figures 1(a) and 11(a), the porous structure formed exclusively on the membrane surface and at the interface of substrate, and no porous structure formed inside the membrane.

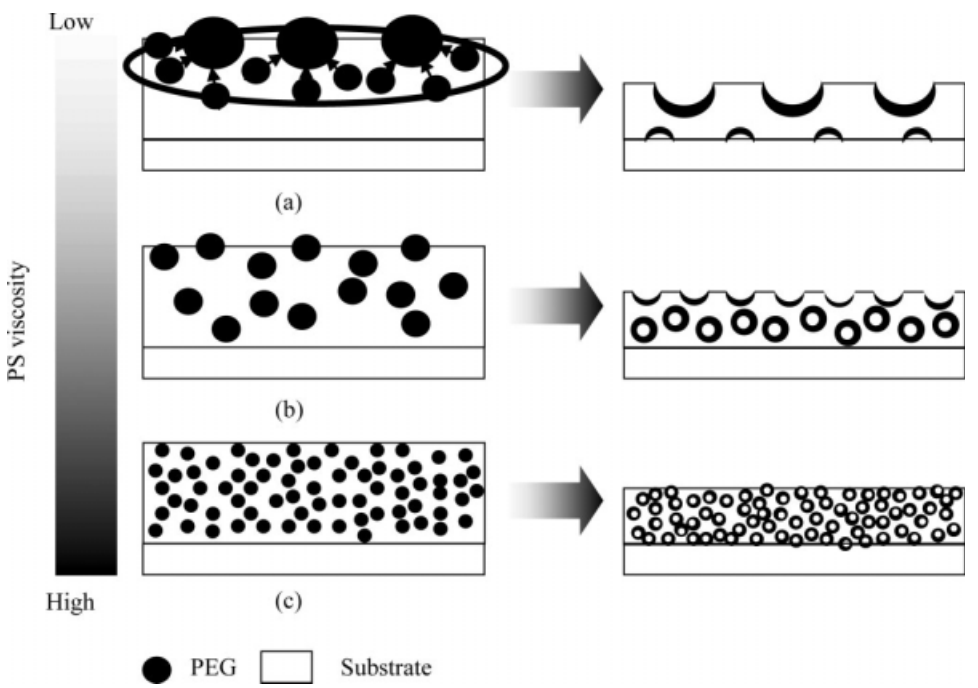

Figure 11 Schematics for the formation process of a fine porous structure in a film.

CONCLUSIONS

A polymeric membrane with a fine porous structure was prepared by the dry-casting of PS and PEG and solvent solutions. By changing the solvent of a PS/PEG blend, we changed the pore size and density as well as the porous structure drastically with the different solvent types and the drying conditions. The increase in the drying rate and the high solubility of PEG in the solvent increased the polymer concentration of the PS-rich phase at the onset of the phase separation of PEG. The higher concentration and higher viscosity of PS at the onset of the PEG phase separation may have suppressed the growth of the PEG-rich domain, and the phase-separated PEG domains were left on the inside of the membrane, and then, pores were created in the PEG-rich domain by secondary phase separation. Finally, a fine porous structure was formed in the membrane.

As Israelichivili and coworkers[37–39] reported, PEG affected the aggregation of colloidal particles and vesicles. Bormashenko et al.[40] also showed that the content of PEG promoted the formation of a closely packed structure when they made a porous film from a PS solution in chlorinated solvents under a humid atmosphere. Their studies pointed out that PEG promoted aggregation under the presence of water in the solution. In our study, the drying experiments were conducted under a nitrogen purge without humidity. In the presence of water or some humidity in our solutions, the hydrophilicity of PEG affected the aggregation of pores and change the porous structure. The drying experiments of PS/PEG/solvent under the controlled humidity gave us a more interesting porous structure because of the synergetic effects of phase separation and the aggregation of pores.

References

1. Akolekar, D. B.; Hind, A. R.; Bhargava, S. K. J Colloid Interface Sci 1998, 199, 92.
2. Lin, V. S. Y.; Motesharei, K.; Dancil, K. P. S.; Sailor, M. J.; Ghadiri, M. R. Science 1997, 278, 840.
3. Nishikawa, T.; Nonomura, M.; Arai, K.; Hayashi, J.; Sawadaishi, T.; Nishiura, Y.; Hara, M.; Shimomura, M. Langmuir 2003, 19, 6193.
4. Hedrick, J. L.; Miller, R. D.; Hawker, C. J.; Carter, K. R.; Volksen, W.; Yoon, D. Y.; Trollsas, M. Adv Mater 1998, 10, 1049.
5. Gineste, J. L.; Pourcelly, G. J Membr Sci 1995, 107, 155.
6. Liu, Y.; Li, K. J Membr Sci 2005, 259, 47.
7. Sadeghi, F.; Ajji, A.; Carreau, P. J. J Membr Sci 2007, 292, 62.
8. Taki, K.; Nitta, K.; Kihara, S. I.; Ohshima, M. J Appl Polym Sci 2005, 97, 1899.
9. Barton, B. F.; Graham, P. D.; McHugh, A. J. J Polym Sci Part B: Polym Phys 1999, 37, 1461.
10. Tsay, C. S.; McHugh, A. J. J Polym Sci Part B: Polym Phys 1990, 28, 1327.
11. Matsuyama, H.; Teramoto, M.; Uesaka, T. J Membr Sci 1997, 135, 271.
12. Yamamura, M.; Nishio, T.; Kajiwara, T.; Adachi, K. Drying Technol 2001, 19, 1397.
13. Kumacheva, E.; Li, L.; Winnik, M. A.; Shinozaki, D. M.; Cheng, P. C. Langmuir 1997, 13, 2483.
14. Affrossman, S.; Kiff, T.; O'Neill, S. A.; Pethrick, R. A.; Richards, R. W. Macromolecules 1999, 32, 2721.
15. Khalil, E. M.; Mohamed, B.; Mosto, B. J Colloid Interface Sci 2007, 306, 354.
16. Liu, T.; Ozisik, R.; Siegel, R. W. Thin Solid Films 2007, 515, 2965.
17. Prosycevas, I.; Amulevicius, S. T.; Guobiene, A. Thin Solid Films 2004, 453, 304.
18. Bergues, B.; Lekki, J.; Budkowski, A.; Cyganik, P.; Lekka, M.; Bernasik, A., Rysz, J.; Postawa, Z. Vacuum 2001, 63, 297.
19. Cyganik, P.; Bernasik, A.; Budkowski, A.; Bergues, B.; Kowalski, K.; Rysz, J.; Lekki, J.; Lekka, M.; Postawa, Z. Vacuum 2001, 63, 307.
20. Chang, L. L.; Woo, E. M. Polymer 2003, 44, 1711.
21. Cui, L.; Han, Y. Langmuir 2005, 21, 11085.
22. Walheim, S.; Boltau, M.; Mlynek, J.; Krausch, G.; Steiner, U. Macromolecules 1997, 30, 4995.
23. Nakane, K.; Hata, Y.; Morita, K.; Ogihara, T.; Ogata, N. J Appl Polym Sci 2004, 94, 965.
24. Kim, W. K.; Char, K.; Kim, C. K. J Polym Sci Part B: Polym Phys 2000, 38, 3042.
25. Mitov, Z.; Kumacheva, E. Phys Rev Lett 1998, 81, 3427.
26. Siggia, E. D. Phys Rev A 1979, 20, 595.
27. Furukawa, H. Phys Rev A 1987, 36, 2288.
28. Song, S. W.; Torkelson, J. M. J Membr Sci 1995, 98, 209.
29. Dekeyser, C. M.; Biltresse, S.; Marchand-Brynaert, J.; Rouxhet, P. G.; Dupont-Gillain, C. C. Polymer 2004, 45, 2211.
30. Bormashenko, E.; Pogreb, R.; Musin, A.; Stanevsky, O.; Bormashenko, Y.; Whyman, G.; Gendelman, O.; Barkay, Z. J Colloid Interface Sci 2006, 297, 534.
31. Kim, J.-K.; Taki, K.; Ohshima, M. Langmuir 2007, 23, 12397.
32. Cui, L.; Wang, H.; Ding, Y.; Han, Y. C. Polymer 2004, 45, 8139.
33. Cha, B. J.; Char, K.; Kim, J. J.; Kim, S. S.; Kim, C. K. J Membr Sci 1995, 108, 219.
34. Mark, J. E. Physical Properties of Polymers Handbook; Springer: New York, 1996.
35. Brandrup, J.; Immergut, E. H. Polymer Handbook, 3rd ed.; Wiley-Interscience: New York, 1989.
36. Kia, S.; Samuel, H. Y. AAPS Pharm Sci Technol 2006, 7, E26.
37. Kuhl, T. L.; Berman, A. D.; Hui, S. W.; Israelichvili, J. B. Macromolecules 1998, 31, 8250.
38. Kuhl, T. L.; Berman, A. D.; Hui, S. W.; Israelichvili, J. B. Macromolecules 1998, 31, 8258.
39. Kuhl, T. L.; Gou, Y.; Alderfer, J. L.; Berman, A. D.; Leckband, D.; Israelichvili, J. B.; Hui, S. W. Langmuir 1996, 12, 3003.
40. Bormashenko, E.; Malkin, A.; Musin, A.; Bormashenko, Y.; Whyman, G.; Litvak, N.; Barkay, Z.; Machavariani, V. Macromol Chem Phys 2008, 209, 567.